# High-Resolution Raman Spectra with Femtosecond Pulses: An Example of Combined Time- and Frequency-Domain Spectroscopy

Sukhendu Nath, Diana C. Urbanek, Sean J. Kern, and Mark A. Berg*

*Department of Chemistry and Biochemistry, University of South Carolina, Columbia, South Carolina 29208, USA*

(Received 1 July 2006; published 28 December 2006; publisher error corrected 21 March 2007)

Frequency-domain spectroscopy requires long pulses, whereas time-domain spectroscopy requires short pulses. This Letter demonstrates both theoretically and experimentally that simultaneous detection in frequency and time generates well-resolved spectra using intermediate-length pulses. In the case of coherent Raman spectroscopy, typical femtosecond pulses lie between the time and frequency domains. To demonstrate this method, a high-resolution Raman spectrum of nitrobenzene is obtained from 60 fs pulses. Phase control, pulse shaping, or pulses of widely differing duration are not required.

DOI: 10.1103/PhysRevLett.97.267401 PACS numbers: 78.47.+p, 33.20.Fb, 42.65.Dr, 82.53.−k

Many new and emerging spectroscopies produce vibrational coherences and then detect them through coherent Raman scattering. Examples include 2D vibrational spectroscopies [1–4], surface-selective, sum-frequency spectroscopies [5,6], Raman-detected, time-resolved photochemistry [7], Raman near-field microscopy [8], tip-enhanced Raman [9,10], vibrationally resolved optical tomography [11] and CARS microscopy [12,13]. Often coherent Raman spectra are measured in the frequency domain by scattering from a nanosecond or longer pulse with a well-defined frequency. However, moving to femtosecond pulses offers many potential advantages: (i) The nonresonant electronic background, which is strong, but instantaneous, can be discriminated from the vibrational coherences, which are weaker, but longer lived. (ii) The signal size is increased by the high peak intensity of short pulses. (iii) The number of interfering coherence pathways is reduced when the pulses have a definite time ordering. (iv) The time-resolution can be increased until it is limited by the intrinsic physics of the sample, rather than by the instrument. (v) Vibrations over a broad spectral region can be excited simultaneously.

However, femtosecond coherent Raman falls in a gap between standard time-domain and frequency-domain spectroscopies. To fully resolve vibrational linewidths in a frequency-domain measurement requires a pulse bandwidth of less than a few wave numbers and therefore a duration of 10 ps or longer. Important vibrations have frequencies as high as 3300 $cm^{-1}$ and therefore periods as short as 10 fs. In time-domain (impulsive) Raman [14,15], pulses of only a few fs are needed to fully resolve such oscillations.

This problem with femtosecond coherent Raman is just one example of a problem that affects all spectroscopies: Spectra can be taken in the time domain using pulses longer than the inverse of the finest feature in the spectrum, and spectra can be taken in the time domain using pulses shorter than the inverse of the highest frequency in the spectrum, but there is a significant gap between these two limits. A general method for taking spectra with intermediate pulse lengths has not been established. In this Letter, we demonstrate a general solution to this problem through combined time and frequency detection (TFD). The experimental feasibility and robustness of this method are demonstrated by recovering a fully resolved CARS spectrum from nitrobenzene using 60 fs pulses.

A number of approaches have been proposed to incorporate ultrafast pulses into coherent Raman measurements. Most of these methods either limit the pulses to picosecond durations [2,9,13] or combine a picosecond-long pulse (or pulse train) with a femtosecond pulse [4,5,7,16–21]. Many of these methods also require careful manipulation of the pulse phases [11,17–21] or relatively difficult heterodyne detection [11,13,21]. All of these methods achieve adequate spectral resolution. However, they also increase the experimental complexity substantially and still miss some of the advantages of femtosecond pulses listed above.

Bordenyuk and Benderskii recently measured TFD data in a surface-sum-generation experiment and directly modeled the vibrational response of water at a $CaF_2$ interface [6]. However, they did not discuss the general problem of inverting TFD data to a high-resolution Raman spectrum as we do here.

In a frequency-domain experiment, one measures the susceptibility $\hat{\chi}(\omega)$, or one of its components, $\mathrm{Im}\hat{\chi}(\omega)$ or $|\hat{\chi}(\omega)|$. In a time-domain experiment, one measures the inverse Fourier transform of this susceptibility, the Raman response-function $\chi(t)$ (also called the free-induction decay). In a coherent Raman experiment, the vibrations are first excited by some sequence of pulses that varies with the specific experiment. These excitation pulses create an effective force $F(t;\tau'/\omega')$ on the vibration at time $t$. Here $\tau'/\omega'$ represents one or more variables within the excitation sequence. These excitation variables can be in either the time or frequency domain. The various time- versus frequency-domain approaches to exciting the vibrational coherence [3] should be distinguished from the time- versus frequency-domain methods of detecting the coherence that are discussed here.

 

After the coherence is prepared, a probe pulse with electric field $E_{\mathrm{pr}}(t)$ scatters from the vibrational coherence to produce anti-Stokes (or Stokes) light of intensity $S_{\mathrm{TF}}$. In a TFD experiment, the anti-Stokes light is both dispersed in frequency $\omega$ and measured as a function of time delay $\tau$ between the final excitation pulse and the probe pulse,

$$S_{\mathrm{TF}}(\tau,\omega)=\frac{1}{2\pi}\left|\int_{-\infty}^{\infty}E_{\mathrm{pr}}(t-\tau)e^{-i\omega t}\times\int_{-\infty}^{t}\chi(t-t')F(t';\tau'/\omega')dt'dt\right|^{2}. \quad (1)$$

The first major point of this Letter is that Eq. (1) can be exactly inverted to recover $\hat{\chi}(\omega)$. In other words, data collected as a function of both time and frequency have complete information on the spectrum. A specific sequence of Fourier manipulations to accomplish the inversion is detailed in the supplemental material [22]. This inversion gives both the amplitude and the phase of the Raman spectrum, even without heterodyne detection. This result is the formal solution of the problem of taking spectra with pulses whose length is between the limits of simple time- or frequency-domain methods.

The remainder of the Letter looks at whether the recovery of spectra from TFD data is practical and robust under realistic experimental conditions. In addition to an explicit recovery of the Raman spectrum of nitrobenzene, we also examine where the essential information resides within the TFD data and discuss which elements of the spectrum will be more or less susceptible to experimental noise.

In our experiments, stimulated Raman generated the vibrational coherence. Thus,

$$F(t,\tau')=E_L(t)E_S(t-\tau'), \quad (2)$$

where $E_L$ and $E_S$ are the Laser and Stokes electric fields, respectively. The Laser and Stokes pulses were centered at 520 and 555 nm, respectively, and excited vibrations within an approximately 500 $\mathrm{cm}^{-1}$ wide band centered at 1200 $\mathrm{cm}^{-1}$. The probe pulse was centered at 800 nm. All pulses were approximately 60 fs long. More detail is given in the supplemental material [22].

The anti-Stokes beam was spatially separated from the other beams and was dispersed in a CCD-based spectrometer. The detection frequency $\omega$ formed the frequency axis. The delay between Laser and Stokes $\tau'$ was adjusted to maximize the signal and then was left unchanged. The time delay of the probe pulse relative to the other pulses $\tau$ was varied to form the time axis.

In the TFD approach, either control or measurement of the pulse phases is beneficial, but not essential. To demonstrate this fact, the current experiments are performed without any phase control after the amplifier. The pulses have both chirp and higher order phase distortions at the sample [22].

Figure 1 shows TFD data from nitrobenzene. Near $\tau = 0$, the nonresonant background creates an intense signal. At later times (above the black curve), the signal is only due to the resonant scattering from the vibrational coherences. Four major Raman bands lie within the excitation region [Fig. 3(a)]. Interference between the scattering from each of these bands leads to a complex pattern of beating throughout the resonant portion of the data. Because of the femtosecond time resolution, the resonant signal can be cleanly separated from the nonresonant signal, even though the peak nonresonant signal is 30 times stronger than the peak resonant signal.

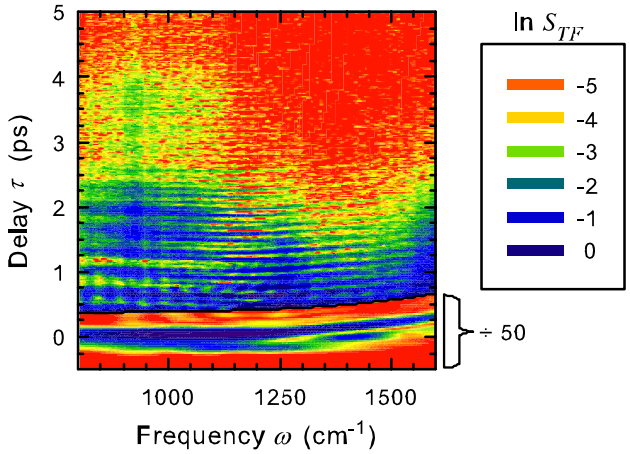


FIG. 1 (color online). Time- and frequency-detected (TFD) coherent anti-Stokes scattering data from nitrobenzene. The natural log of the signal intensity, ln $S_{\mathrm{TF}}(\tau,\omega)$, is plotted out-of-plane. The black curve, $T(\omega)$ + 350 fs [22], is used to cut off the nonresonant signal at short times. The signal intensity below this curve is divided by 50.

Figure 2 shows that one-dimensional information alone is insufficient to recover the Raman spectrum. If the TFD data are integrated over all time, the result is dominated by the nonresonant signal [Fig. 2(a), dashed]. If the nonresonant signal is removed by cutting off the short-time data [22], the time-integrated resonant spectrum is broader than the pulse spectrum [Fig. 2(a), dot-dashed], showing that there are multiple lines in the spectrum. However, these lines are completely unresolved [Fig. 2(a), solid].

Figure 2(b) (total) shows the TFD data integrated over frequency. This curve replicates a time-resolved CARS experiment without frequency selection of the anti-Stokes light. A sense of the extra information available in the TFD data can be gained by looking at several cuts at specific frequencies. The many different oscillations that overlap in the frequency-integrated experiment are separated in the TFD data.

A more intuitive picture of the data results from Fourier transforming $S_{\mathrm{TF}}(\tau,\omega)$ along the time axis to yield a frequency-frequency representation $S_{\mathrm{FF}}(\delta\omega,\omega)$. Before this transform is made, we cut off the nonresonant signal below the black curve in Fig. 1 [22]. The nitrobenzene data in this frequency-frequency representation are shown in Fig. 3(b).

The TFD data in the frequency-frequency representation consist of a series of bands that are narrow along $\delta\omega$, but broad in $\omega$. The peaks of these bands along the new frequency variable $\delta\omega$ indicate the splittings, $\nu_i - \nu_j$, between lines in the Raman spectrum. The widths along the $\delta\omega$ axis are determined by the natural linewidths of the Raman bands, allowing the frequency splittings to be determined with high accuracy. The Raman line shapes are accurately determined by fitting the peaks along this dimension, or equivalently by fitting the time decays in the time-frequency representation.

The peaks are located along the $\omega$ axis at the (weighted) average of the frequencies of the bands involved in the splitting. Along this dimension, the width is determined by the frequency width of the probe spectrum. This width is too broad to provide accurate frequency information. However, the position along $\omega$ does indicate the approximate position of the frequency splitting within the spectrum. This information is sufficient to remove the ambiguities that can arise in trying to reconstruct a spectrum from a list of frequency splittings alone.

To model the TFD data, we use Eq. (1) and represent the Raman susceptibility by

$$\chi(t) = \sum_{i=1}^{n} A_i \sin(\nu_i t) e^{-t/T_{2i}}, \tag{3}$$

where the line amplitudes, frequencies, and dephasing times (linewidths) are given by $A_i$, $\nu_i$, and $T_{2i}$, respectively. The coherence decays are represented by exponentials in the time domain, or equivalently, the Raman lines are represented by Lorentzians in the frequency domain. The line shape is fully determined by the TFD data. An exponential model was used because visual inspection of the data shows that it would fit the data well [Fig. 2(b)]. The light pulses are modeled as bandwidth limited, flat-phase Gaussians with intensity FWHM of 56 fs for the Laser and Stokes and 50 fs for the probe.

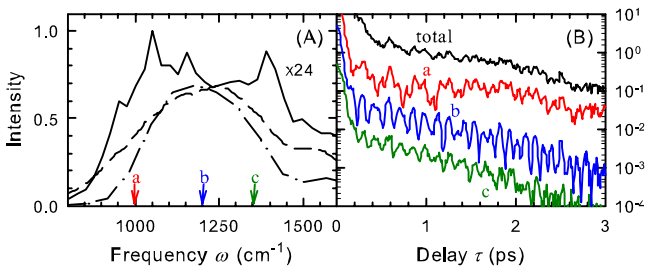


FIG. 2 (color online). One-dimensional subsets of the full TFD data. (a) Dashed: integrated over all time. Solid: integrated after cutting off the nonresonant signal at short time (×24). Dash-dotted: Spectrum of the probe pulse. (b) Solid: integrated over all frequencies (total, black). Slices in time at specific frequencies (integrated over ±50 cm$^{-1}$): 1000 cm$^{-1}$ (*a*, red), 1200 cm$^{-1}$ (*b*, blue) and 1350 cm$^{-1}$ (*c*, green).

The model of the TFD signal in the frequency-frequency representation [Fig. 3(c)] reproduces the important features of the data. It yields the Raman spectrum in Fig. 3(d), which can be compared to the spontaneous Raman spectrum in Fig. 3(a).

By comparing the frequency-frequency data [Fig. 3(b)] to the spectrum recovered from the model [Fig. 3(d)], it is easy to see where the information needed to reconstruct the spectrum comes from. There are six frequency splittings among the four major Raman bands. Each peak along the $\delta\omega$ axis in the TFD data is easily assigned to one of these splittings. These peaks only indicate the magnitude of the splitting, not its sign. As a result, one peak by itself (e.g., **e**: $\nu_4 - \nu_3$) does not indicate which of the bands is to the high frequency side of the other band. However, other splittings from each of the bands to a third band (e.g., **a**: $\nu_4 - \nu_1$ and **b**: $\nu_3 - \nu_1$) provide a unique ordering.

From the preceding discussion, we see that the TFD approach yields accurate values for line shapes, linewidths, and frequency separations. These values derive from clearly observable features of the data, and so the recovery of the Raman spectrum from TFD data will be accurate and robust. In particular, these values are not highly sensitive to the detailed structure of the light pulses.

The absolute frequencies have a greater error than the frequency splittings. The absolute frequency scale is measured from the shift between the probe spectrum and the anti-Stokes peak along the broad $\omega$ dimension. In Fig. 3, the frequency axis has been shifted slightly to match the known Raman spectrum. If this shift needs to be deter-

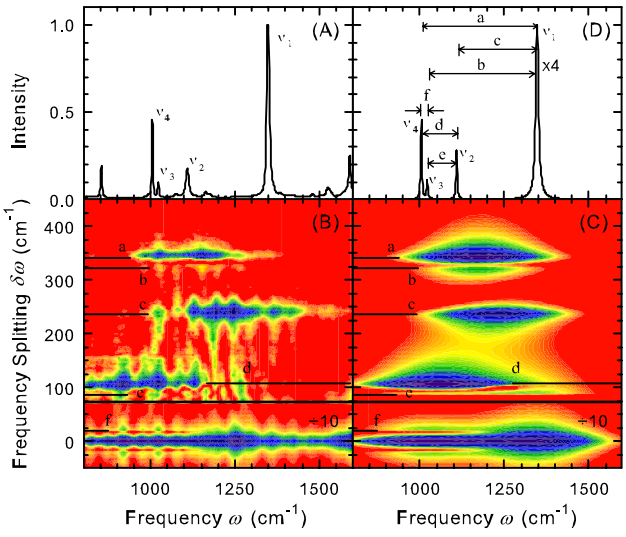


FIG. 3 (color online). Raman data from nitrobenzene. (a) Spontaneous Raman spectrum. Natural log of the TFD experimental (b) and theoretical (c) data in the frequency-frequency representation, ln $S_{\mathrm{FF}}(\delta\omega, \tau)$. Signals below the line at 70 cm$^{-1}$ have been divided by 10. Labeled lines ($a$–$f$) indicate the peaks corresponding to frequency splittings in the Raman spectrum (see *d*). (d) Raman spectrum, Im $\hat{\chi}(\omega)$, recovered from the model.

mined independently, a standard with a known Raman line can be added to the sample.

As in any coherent Raman spectroscopy, the amplitudes of the lines are a product of the spontaneous Raman cross section and the excitation intensity. In Fig. 3(d), the $\nu_1$ line is near the edge of the excitation band and as a result, it is smaller than in the spontaneous Raman spectrum.

Careful control or measurement of the pulse phases was not used here and is not essential to TFD spectroscopy. However, it does offer potential improvements. With phase information on the pulses, it should be possible to recover the phase of the Raman spectrum, in addition to the magnitude that was recovered here. Phase information on the Raman spectrum would allow resolution of dynamics faster than the vibrational dephasing times [7].

The frequency resolution of the recovered Raman spectrum is formally determined by the inverse of the time range of the TFD data. However, this range is easily adjusted to match the range over which signal is detectable. If the signal is strong enough to measure coherence decays over a few lifetimes, the frequency resolution is determined only by the natural Raman linewidths, not by instrumental factors.

In summary, the simultaneous collection of data in time and frequency is an effective method of performing spectroscopy with pulse durations that lie between the limiting cases of time-domain and frequency-domain spectroscopy. In the case of coherent Raman, recovery of the spectrum from TFD data is not highly sensitive to experimental noise or to imperfections in pulse properties. The frequency resolution is limited only by the natural linewidths (1–10 $cm^{-1}$), even when using 60 fs pulses, which have a bandwidth of $>300$ $cm^{-1}$.

We thank William F. Pearman for assistance with the spontaneous Raman spectrum. This Letter was supported by the National Science Foundation through Grant No. CHE-0210986 with major equipment support from Grant No. MRI-0216056.

*Email address: berg@mail.chem.sc.edu

[1] W. Zhao and J. C. Wright, Phys. Rev. Lett. **84**, 1411 (2000).
[2] K. A. Meyer and J. C. Wright, Anal. Chem. **73**, 5020 (2001).
[3] A. V. Pakoulev, M. A. Rickard, K. A. Meyer, K. Kornau, N. A. Mathew, D. E. Thompson, and J. C. Wright, J. Phys. Chem. A **110**, 3352 (2006).
[4] P. Kukura, R. Frontiera, and R. A. Mathies, Phys. Rev. Lett. **96**, 238303 (2006).
[5] L. J. Richter, T. P. Petralli-Mallow, and J. C. Stephenson, Opt. Lett. **23**, 1594 (1998).
[6] A. N. Bordenyuk and A. V. Benderskii, J. Chem. Phys. **122**, 134713 (2005).
[7] P. Kukura, D. W. McCamant, S. Yoon, D. B. Wandschneider, and R. A. Mathies, Science **310**, 1006 (2005).
[8] R. D. Schaller, J. Ziegelbauer, L. F. Lee, L. H. Haber, and R. J. Saykally, J. Phys. Chem. B **106**, 8489 (2002).
[9] T. Ichimura, N. Hayazawa, M. Hashimoto, Y. Inouye, and S. Kawata, Phys. Rev. Lett. **92**, 220801 (2004).
[10] A. Hartschuh, E. J. Sanchez, X. S. Xie, and L. Novotny, Phys. Rev. Lett. **90**, 095503 (2003).
[11] D. L. Marks and S. A. Boppart, Phys. Rev. Lett. **92**, 123905 (2004).
[12] A. Zumbusch, G. R. Holtom, and X. S. Xie, Phys. Rev. Lett. **82**, 4142 (1999).
[13] E. O. Potma, C. L. Evans, and X. S. Xie, Opt. Lett. **31**, 241 (2006).
[14] L. Dhar, J. A. Rogers, and K. A. Nelson, Chem. Rev. **94**, 157 (1994).
[15] J. P. Ogilvie, E. Beaurepaire, A. Alexandrou, and M. Joffre, Opt. Lett. **31**, 480 (2006).
[16] T. W. Kee and M. T. Cicerone, Opt. Lett. **29**, 2701 (2004).
[17] K. P. Knutsen, J. C. Johnson, A. E. Miller, P. B. Petersen, and R. J. Saykally, Chem. Phys. Lett. **387**, 436 (2004).
[18] E. Gershgoren, R. A. Bartels, J. T. Fourkas, R. Tobey, M. M. Murnane, and H. C. Kapteyn, Opt. Lett. **28**, 361 (2003).
[19] N. Dudovich, D. Oron, and Y. Silberberg, Nature (London) **418**, 512 (2002).
[20] T. Hellerer, A. M. K. Enejder, and A. Zumbusch, Appl. Phys. Lett. **85**, 25 (2004).
[21] B. Yellampalle, R. D. Averitt, A. Efimov, and A. J. Taylor, Opt. Express **13**, 7672 (2005).
[22] See EPAPS Document No. E-PRLTAO-97-025702 for more details of the experiment and analysis. For more information on EPAPS, see http://www.aip.org/pubservs/epaps.html